Wear and Wear Mechanism Simulation of Heavy-Duty Engine Intake Valve and Seat Inserts

Y.S. Wang, S. Narasimhan, J.M. Larson, and S.K. Schaefer

(Submitted 21 May 1997; in revised form 7 October 1997)

A silicon-chromium alloy frequently used for heavy-duty diesel engine intake valves was tested against eight different insert materials with a valve seat wear simulator. Wear resistance of these combinations was ranked. For each test, the valve seat temperature was controlled at approximately 510 °C, the number of cycles was 864,000 (or 24 h), and the test load was 17,640 N. The combination of the silicon-chromium valve against a cast iron insert produced the least valve seat wear, whereas a cobalt-base alloy insert produced the highest valve seat wear. In the overall valve seat recession ranking, however, the combination of the silicon-chromium valve and an iron-base chromium-nickel alloy insert had the least total seat recession, whereas the silicon-chromium valve against cobalt-base alloy, cast iron, and nickel-base alloy inserts had significant seat recession. Hardness and microstructure compatibility of valve and insert materials are believed to be significant factors in reducing valve and insert wear.

The test results indicate that the mechanisms of valve seat and insert wear are a complex combination of adhesion and plastic deformation. Adhesion was confirmed by material transfer, while plastic deformation was verified by shear strain (or radial flow) and abrasion. The oxide films formed during testing also played a significant role. They prevented direct metal-to-metal contact and reduced the coefficient of friction on seat surfaces, thereby reducing adhesive and deformation-controlled wear.

Keywords engine valve seat wear, heavy-duty engine valve, seat wear simulation, wear mechanism

1. Introduction

Engine valve seat wear is one of the most important factors affecting engine performance. Because of higher performance demands and the increasing use of alternative fuels, engine intake valve seats are challenged with greater wear problems than in the past. Valve manufacturers are continuously working with engine manufacturers to improve valve quality and life. Many changes in material, design, and construction have greatly improved engine valve and engine performance. However, these changes have difficulty keeping pace with the demands placed on engine valves due to continually increasing performance requirements in the competitive world market.

Y.S. Wang, S. Narasimhan, J.M. Larson, and **S.K. Schaefer,** Eaton Corporation, Engine Components Operations, 19218 B Drive South, Marshall, MI 49068, USA.

Exhaust valves in heavy-duty diesel engines have less serious seat wear problems than do intake valves. Exhaust gas always contains some oil mist and soot, which may have a lubricating effect. It is believed that a coating is usually formed on the exhaust valve seat; though very thin, this coating can be very effective in protecting valve seats from wear damage. Intake valve seats, however, usually show a bright metal surface due to lack of lubrication and have severe seat wear problems (Ref 1, 2). Intake valve seat wear is generally thought to occur by three types of wear: adhesive wear, abrasive wear, and plastic deformation controlled wear (Ref 3-5).

Engine design, environment, manufacture, and maintenance all contribute significantly to valve life (Ref 6). In addition, valve and insert materials, as well as the pairing of valve/seat inserts, are critical to the successful reduction of valve and seat insert wear (Ref 7). Currently, a silicon-chromium steel, commonly known as Sil 1, is used as an intake valve material against different insert materials in heavy-duty diesel engine applications (Table 1). This question is often raised: Which valve and insert combination has the least valve seat recession (valve plus insert

Table 1 Nominal chemical compositions, microstructure, hardness, and applications of the tested heavy-duty engine intake valve/insert materials

	Composition, wt%							Microstructure and hardness,	
Material	C	Mn	Si	Cr	Ni	Fe	Other	HRC	Applications
Sil 1	0.45	0.40	3.20	8.5	0.40	bal	…	Carbide + ferrite, 43 ± 3	Intake valve
Sil XB	1.50	0.40	2.15	20.0	1.30	bal	…	Carbide + ferrite, 42 ± 2	Intake aircraft valve, insert
PL 7	3.14	0.67	1.94	0.61	0.83	bal	Mo, 1.12	Graphite + ferrite + carbide, 42 ± 2	Insert
Stellite 3	2.40	1.0	1.0	31.0	3.0	3.0	Co, bal; W, 12.5	Carbide + solid solution, 54 ± 2	Facing, insert
PL 33	2.05	0.60	1.95	34.0	0.5	bal	Mo, 2.25	Carbide + ferrite, 37 ± 3	Insert
Eatonite	2.40	…	1.0	29.0	39.0	8.0	W, 15.0; Co, 10.0	Carbide + solid solution, 42 ± 2	Insert
Eatonite 6	2.0	1.0	1.50	28.0	10.0	bal	Mo, 5.0	Carbide + ferrite, 39 ± 2	Facing, insert
Tribaloy 400	0.08	…	2.6	8.5	…	3.0	Co, bal; Mo, 29	Laves + solid solution, 53 ± 2	Facing, insert
PMF 16	1.0	0.75	…	5.5	…	bal	V, 2.5; W, 6.0	Carbide + ferrite + porosity, 42 ± 2	Insert

seat wear depth)? Simulation tests have been developed and verified to be capable of simulating an engine operating environment (Ref 8).

The objectives of this study were (1) to rank the wear resistance of Sil 1 valves against different insert materials using a simulator; (2) to analyze the different seat wear patterns by using optical microscopy, three-dimensional (3-D) seat wear profiles, scanning electron microscopy (SEM), and energy-dispersive x-ray analysis (EDX); and (3) to determine the seat wear mechanisms. After these combinations are ranked and wear mechanisms are understood, proper seat insert materials can be recommended to run against a Sil 1 valve, so that longer engine intake valve life can be achieved.

2. Experimental Procedures

The valve seat wear simulator is designed to simulate valve seat wear produced in internal combustion engines (Ref 8). However, because it uses a natural gas flame for heating, a simulator does not simulate the chemical wear that is seen on some field-run valves. The simulator consists of three major parts: the hydraulic system, the electronic control system, and the mechanical equipment (Fig. 1a).

The hydraulic actuator is used to apply the load to the valve head to simulate engine combustion pressure. The load versus time varies in a triangular fashion; that is, load reaches a maximum linearly in 0.05 s and reduces to zero in 0.05 s. Loading frequency is 10 Hz, and valve displacement is set at 1.27 mm. The control system is an electronic unit to control and monitor all test parameters, which include load applied on the valve head, spring load, temperatures of the valve and insert, and displacement of the valve. A load cell is used to monitor the mag-

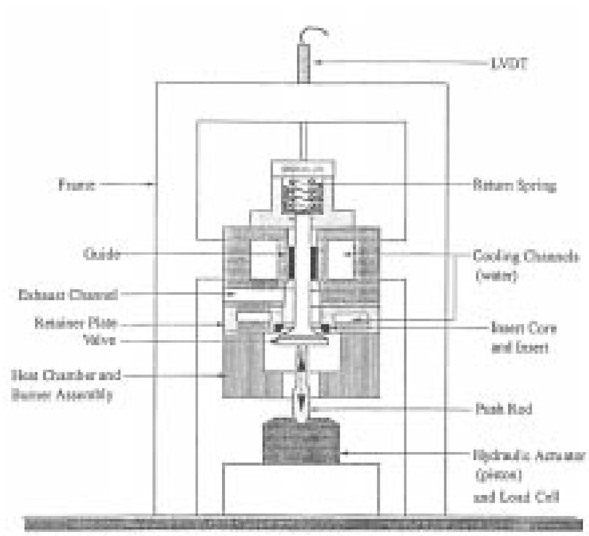

(a)

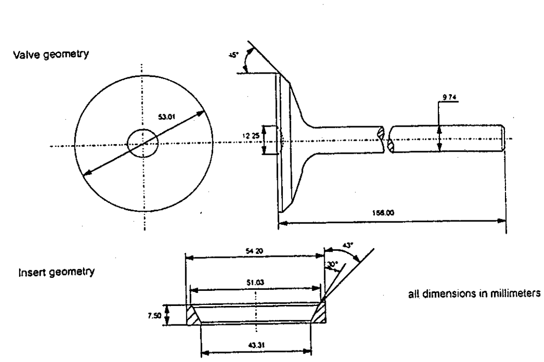

(b)

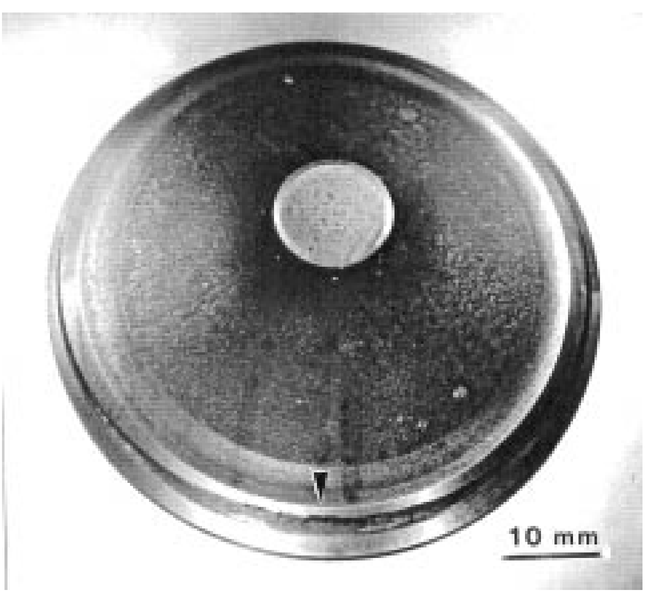

(c)

(d)

Fig. 1 (a) Schematic of the simulator. (b) Valve and seat insert dimensions. (c and d) Macrophotographs of typical tested crescent valve and seat insert wear scars nitude of the seating load, and together with a control loop, a desired load is maintained. A linearly variable differential transformer is used to ensure that the valve does not travel too far off its insert or too far into its insert, which could result in component damage or equipment failure. Sample and system temperatures are monitored using five thermocouples. Two thermocouples are located 180° apart along the valve seat face. Two corresponding thermocouples are located along the seat of the insert. The remaining thermocouple is used to monitor the coolant system.

The tested valves were supplied with the seat premachined to a 45° angle. Production diesel engine valve seat angles are typically machined to 30°. The 45° seat angle creates more radial sliding during valve closing, and thus was chosen as the preferred seat angle for accelerated wear testing of valve seats. The seat of the insert was machined to a 0.51 mm width and a 47° seat angle. The valve and insert geometries and dimensions are shown in Fig. 1(b). The simulator was designed to have a lateral offset of 0.76 mm, which produces a crescent wear scar on the valve seat (Fig. 1c). A profilometer was used to measure valve seat wear at position 3 (indicated by the arrow in Fig. 1c), which has the maximum wear due to the maximum contact stress introduced by the offset. Ten traces, 1° apart, were measured for 3-D plotting. Three-dimensional diagrams of seat

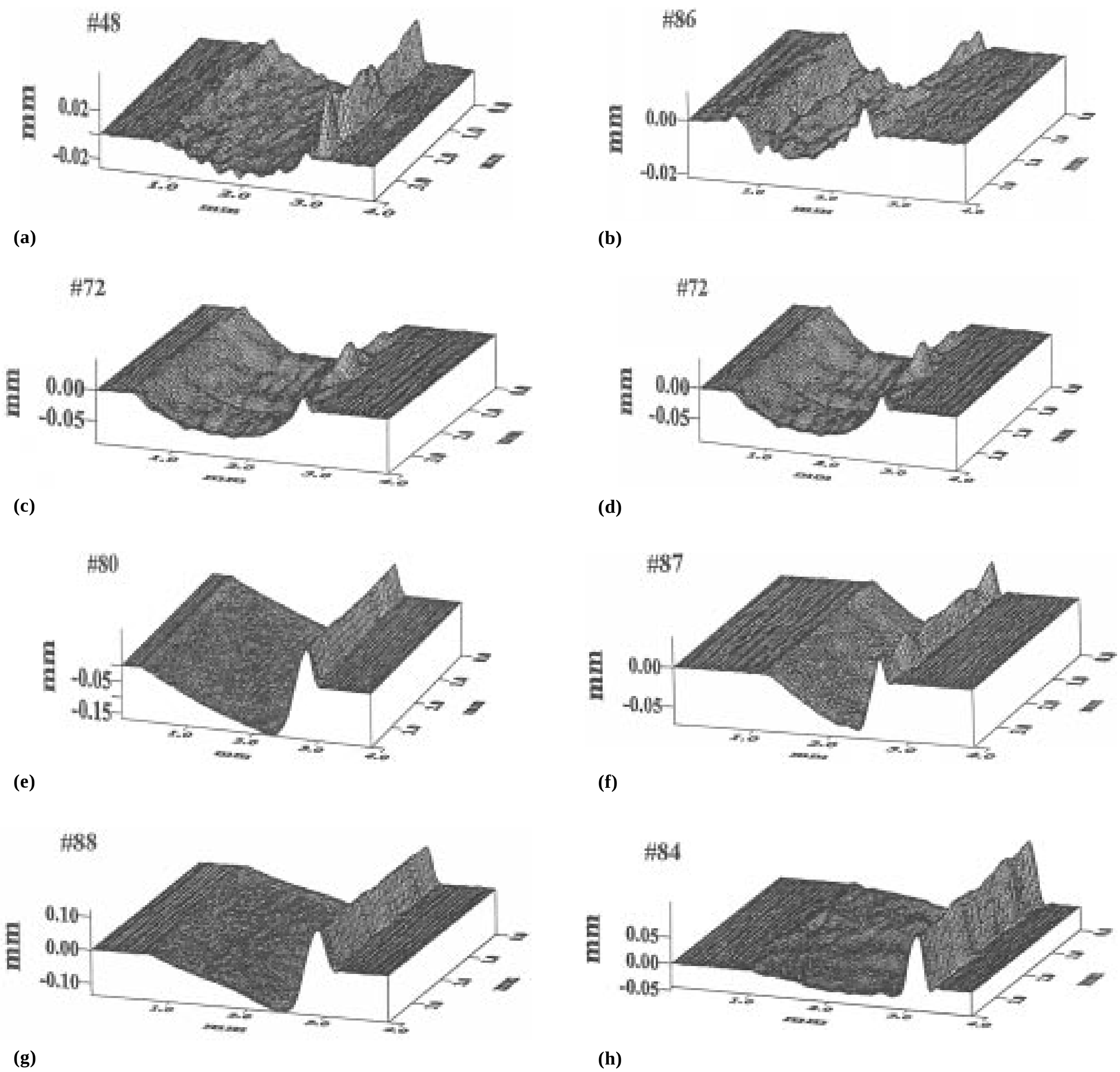

Fig. 2 Three-dimensional valve seat wear scar profiles at the maximum seat wear areas. (a) Sil 1 valve/Sil XB insert. (b) Sil 1 valve/PMF 16 insert. (c) Sil 1 valve/PL 33 insert. (d) Sil 1 valve/PL 7 insert. (e) Sil 1 valve/T 400 insert. (f) Sil 1 valve/Eatonite 6 insert (g) Sil 1 valve/Eatonite insert. (h) Sil valve/Stellite 3 insert

wear scars help to visualize the magnitude and morphology of seat wear patterns. The maximum wear depth and width were measured from 2-D traces and plotted for quantitative comparison.

The valve material was Sil 1, and the insert materials were Sil XB, PL 7, Stellite 3, PL 33, Eatonite, Eatonite 6, Tribaloy 400 (or T 400), and PMF 16. Chemical compositions of valve and seat insert materials are listed in Table 1. Tests were conducted at a temperature of 510 ± 30 °C and a load of 17,640 ± 900 N for 864,000 cycles (24 h). Profilometry was used as the primary method to measure the depth and width of valve seat wear scars. Photography was used to measure the width of the insert seat wear scar, and the insert wear scar depth was estimated from the wear scar width and the unworn geometry of the inserts.

Scanning electron microscopy allowed observation of wear morphologies on the seat, while EDX was used to identify the qualitative chemical composition change during the test (i.e., detection of material transfer). Each valve was examined primarily at the location that underwent maximum contact stress due to lateral misalignment.

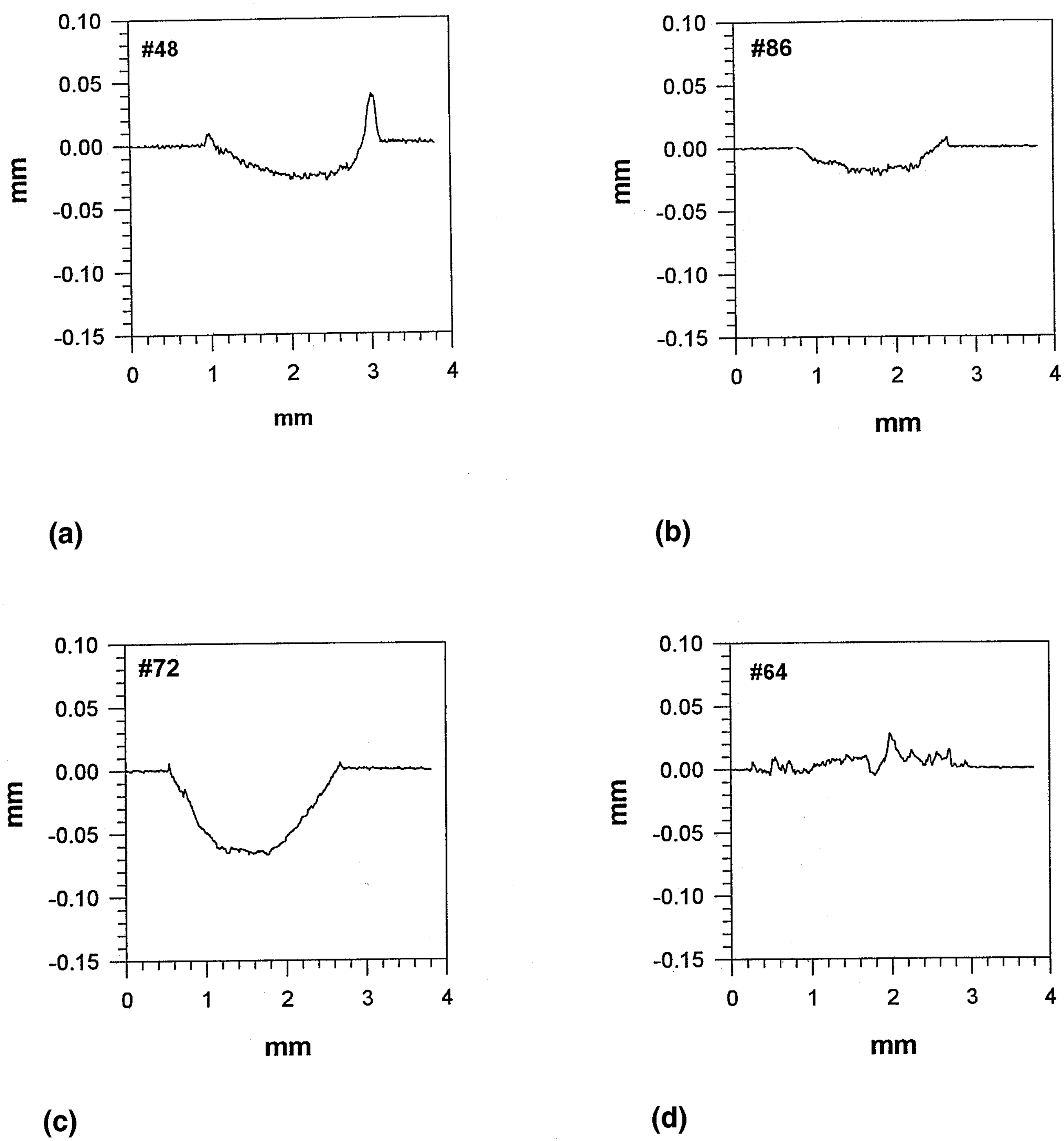

(continued)

Fig. 3 Two-dimensional valve seat wear scar profiles. (a) Sil 1/Sil XB. (b) Sil 1/PMF 16. (c) Sil 1/PL 33. (d) Sil 1/PL 7

3. Results and Discussion

3.1 *Wear Resistance Ranking*

Sil 1 intake valves were tested against eight seat insert materials, with a minimum of three tests conducted for each combination. Table 2 lists the seat wear test matrix and results. Typical 3-D worn surface morphologies of Sil 1 valve seats at the maximum wear region are shown in Fig. 2. The left side of the profiles in Fig. 2 is the minor diameter (ID) of the valve seat, and the right side is the major diameter (OD) of the valve seat.

Figure 3 illustrates 2-D profiles displaying the maximum wear scar depth shown in Fig. 2. The maximum valve seat wear scar depth and width are measured from these traces and plotted in Fig. 4 for comparison.

Figure 4(a) shows the valve seat wear resistance ranking of the Sil 1 valve against PL 7, PMF 16, Eatonite 6, Eatonite, Sil XB, Stellite 3, PL 33, and T 400 inserts. The wear resistance ranking of these combinations is as follows: PL 7 (best), PMF 16, Sil XB, Stellite 3, PL 33, Eatonite 6, Eatonite, and T 400 (worst). Note that the maximum wear scar depth of the Sil 1 valve against the PL 7 insert (0.012 mm) is an order of magni-

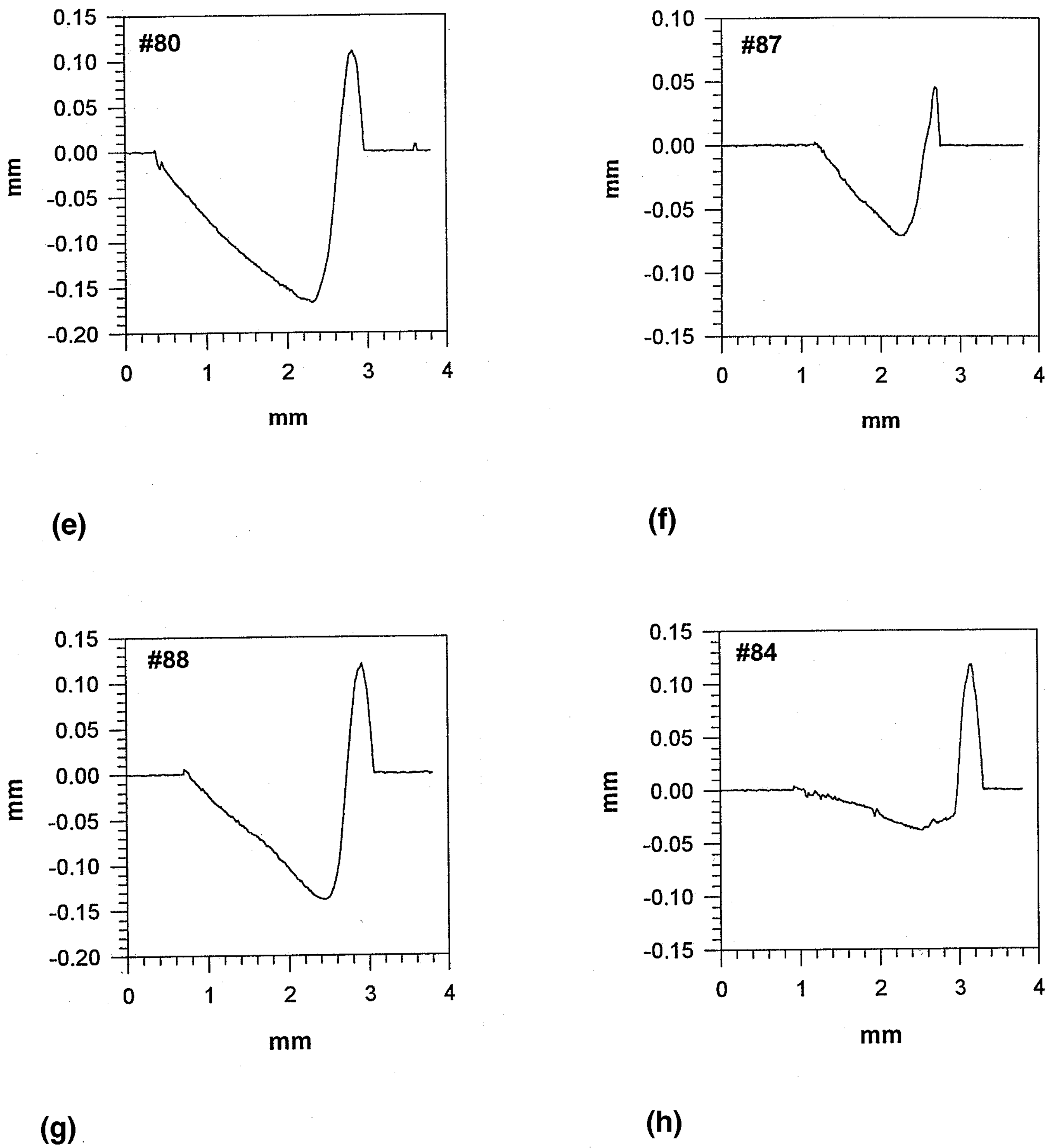

Fig. 3 (cont.) Two-dimensional valve seat wear scar profiles. (e) Sil 1/T 400. (f) Sil 1/Eatonite 6. (g) Sil 1/Eatonite. (h) Sil 1/Stellite 3 tude less than that of the Sil 1 valve against the T 400 insert (0.123 mm). Next to the PL 7 insert, the PMF 16, Sil XB, and Stellite 3 inserts are the most compatible seat inserts against the Sil 1 valve. The Eatonite insert caused the Sil 1 valve to wear as severely as the T 400 insert.

Figure 4(b) shows the wear resistance ranking in terms of valve seat recession (or combined valve seat and insert wear). The lowest total seat recession occurred when the Sil 1 valve was run against the Eatonite 6 insert, followed by the PMF 16, Sil XB, Stellite 3, and PL 33 inserts. T 400, PL 7, and Eatonite inserts exhibited relatively severe seat recessions against the Sil 1 valve. From an economic and wear performance viewpoint, the combinations of a Sil 1 valve and an Eatonite 6 or PMF 16 insert are the best among the eight combinations tested.

Table 2 Valve and seat wear results from simulation tests at 17,640 N and 510 °C for 24 h

Material		Valve seat wear, mm		Insert seat wear, mm		
Valve	Insert	Width	Depth	Width	Depth	Test No.
Sil 1	Sil XB	1.85	0.030	1.80	0.343	18
		1.65	0.027	1.53	0.306	21
		1.45	0.025	1.27	0.269	24
		2.05	0.022	1.83	0.347	30
		1.86	0.028	1.57	0.311	48
		2.24	0.042	2.07	0.381	95
	PMF 16	1.18	0.030	1.13	0.250	27
		1.14	0.009	1.80	0.343	61
		1.70	0.022	1.90	0.357	86
	PL 33	1.31	0.048	1.33	0.278	50
		2.13	0.060	1.80	0.343	68
		2.04	0.059	1.77	0.338	72
	PL 7	1.24	0.007	2.80	0.482	64
		1.38	0.019	2.07	0.381	73
		1.07	0.011	2.17	0.394	89
	T 400	1.83	0.082	1.40	0.288	44
		2.09	0.121	1.50	0.301	56
		2.33	0.167	1.57	0.311	80
	Eatonite 6	1.39	0.086	0.76	0.199	65
		1.46	0.074	0.93	0.222	67
		1.35	0.071	1.13	0.250	87
	Eatonite	2.08	0.095	1.83	0.347	74
		1.95	0.138	1.67	0.325	88
		2.06	0.109	1.67	0.325	96
	Stellite 3	1.92	0.038	2.03	0.375	84
		1.67	0.028	1.83	0.347	90
		1.49	0.039	1.50	0.301	97
T-400-hardfaced Sil 1	Sil XB	2.41	0.140	2.00	0.371	62
		2.38	0.113	1.97	0.367	70
		2.20	0.134	1.93	0.361	93
Sil XB	Sil XB	1.81	0.028	1.87	0.353	85
		1.95	0.029	1.90	0.357	92
		1.95	0.028	1.73	0.333	99

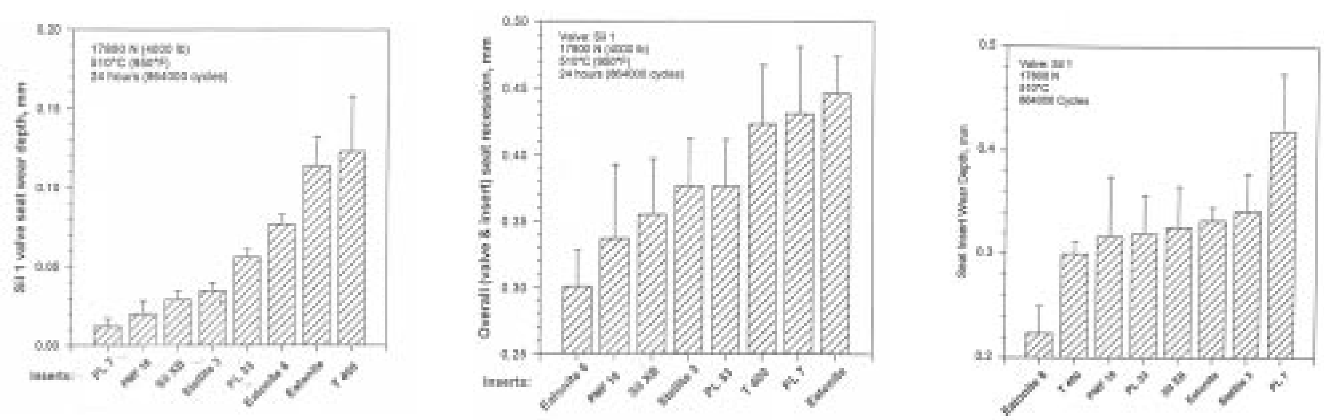

(a) **(b)** **(c)**

Fig. 4 Wear resistance ranking of Sil 1 valve against different seat inserts. (a) Valve seat wear. (b) Total seat recession. (c) Seat insert wear ranking

3.2 *Wear Mechanisms of Valve Seat and Insert*

Valve seat and insert wear mechanisms were a complex combination of shear strain (or radial flow), abrasion, and adhesion. The results of this study indicate that valve seat wear mechanisms depend not only on operating conditions, but also on hardness and the microstructural compatibility of valve and insert materials (Ref 7, 8). Figures 2(a), 2(e) to (h), 3(a), and 3(e) to (h) show valve seat material being pushed up at the OD side of wear scars, which indicates that shear strain or radial flow played a significant role in valve seat wear. Figures 2(d) and 3(d) show material being raised above the valve seat surface inside the wear scar, which indicates that adhesion or material transfer from the seat insert to the valve seat has occurred.

Figure 5 shows the microstructure of the seat inserts at a radial section through the seat after rig testing. The microstructure of the Sil XB insert consists of distributed primary chromium carbides and secondary spheroidized carbides in a ferritic matrix with a hardness of 42 ± 2 HRC (Fig. 5a). The PL 33 insert has primary chromium-molybdenum carbides in a chromium-rich ferritic matrix and a hardness of 37 ± 3 HRC (Fig. 5b). An appreciable amount of oxide film can be seen at the seat surface. The oxide film is believed to protect the seat from direct metal-to-metal contact, thus reducing adhesive

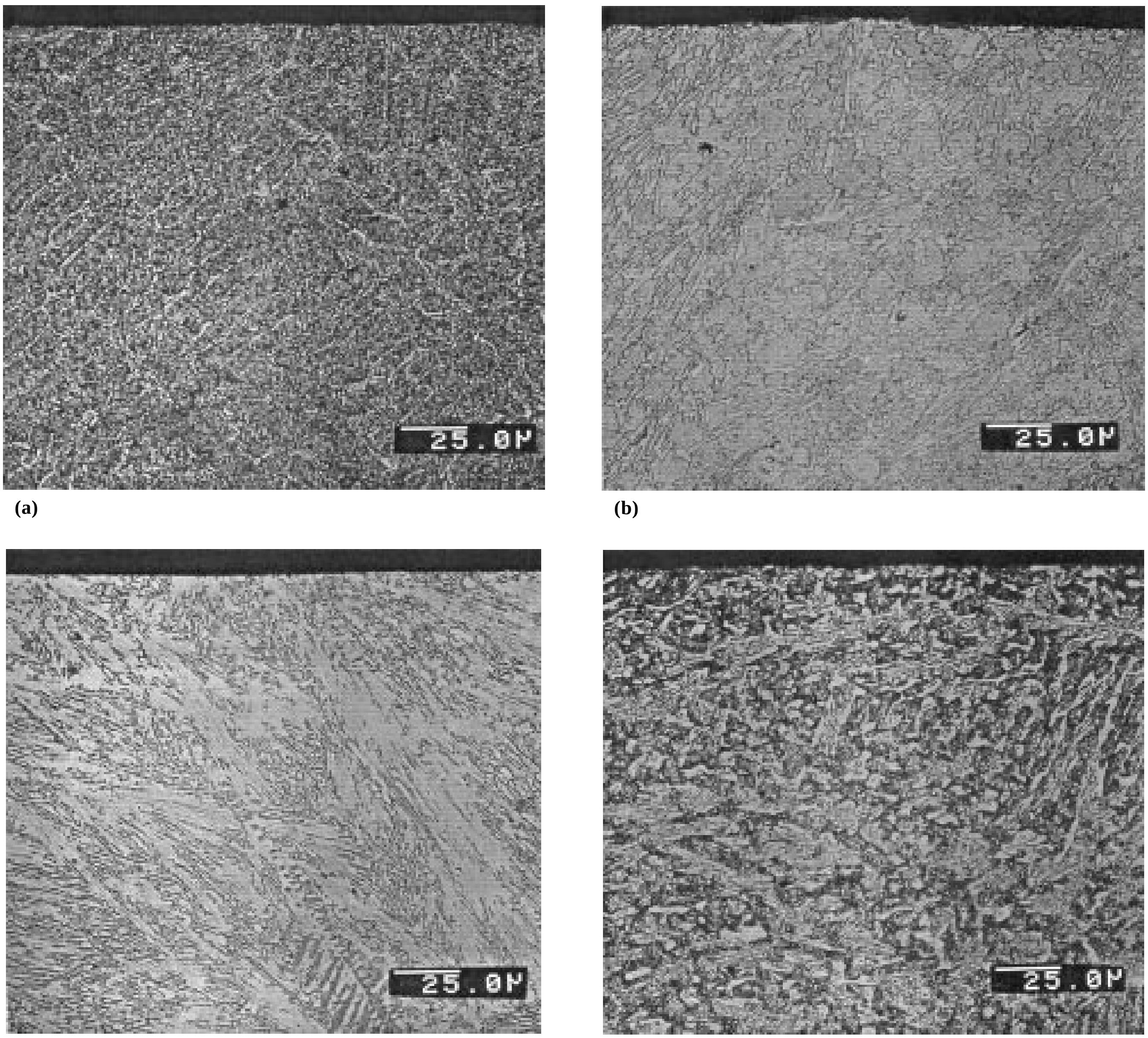

(a) (b) (c) (d)

(continued)

Fig. 5 Microstructures of tested seat inserts at the seat. (a) Sil XB, Vilella's reagent. (b) PL 33, Marble's reagent. (c) Stellite 3, Marble's reagent. (d) Eatonite 6, Marble's reagent wear. The oxide film also reduces the coefficient of friction at the sliding surface, which reduces the shear stress. Therefore, the oxide film helped reduce shear strain-controlled wear.

The Stellite 3 insert has a microstructure of chromium-tungsten-cobalt primary and eutectic carbides within a cobalt solid-solution matrix with a hardness of 54 ± 2 HRC (Fig. 5c). The Eatonite 6 insert has chromium-nickel-molybdenum primary and eutectic carbides evenly distributed in a ferritic matrix with a hardness of 39 ± 2 HRC. Oxide film can be seen on the tested insert seat surface (Fig. 5d). T 400 has a microstructure of Laves phase dispersed in a softer eutectic/solid-solution matrix with a hardness of 53 ± 2 HRC (Fig. 5e).

The Eatonite insert has a microstructure of chromium-tungsten-nickel-cobalt primary and eutectic carbides in a nickel solid-solution matrix with a hardness of 42 ± 2 HRC. The insert seat surface was strained and oxidized (Fig. 5f). PL 7 is a gray cast iron with primary carbide and flake graphite evenly distributed in a ferritic matrix (Fig. 5g). It has a hardness of 42 ± 2 HRC. PMF 16, a powder metal sintered material, has a microstructure of chromium-tungsten-vanadium primary and eutectic carbides plus porosity evenly distributed in a ferritic matrix (Fig. 5h). It has a hardness of 42 ± 2 HRC.

Figure 6 shows the microstructure and seat wear morphologies of radially sectioned Sil 1 valves after rig testing and field engine testing. The Sil 1 valve has a microstructure of evenly distributed fine primary and secondary carbides in a ferritic matrix with a hardness of 43 ± 3 HRC. The common seat wear characteristics among the rig tests and engine test are that the

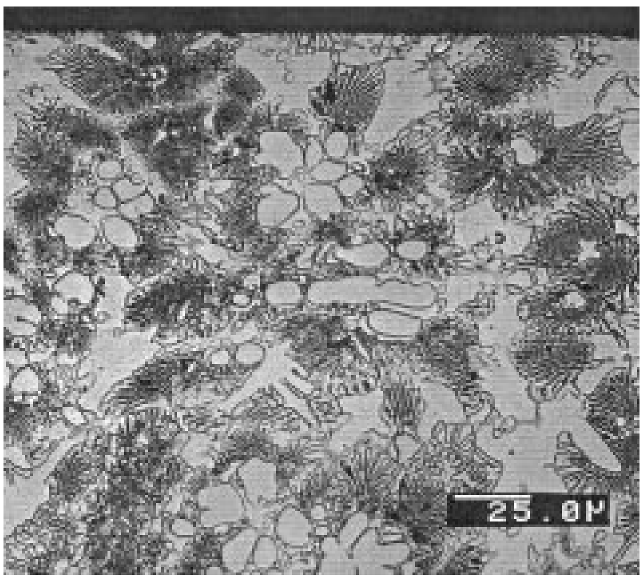

(e)

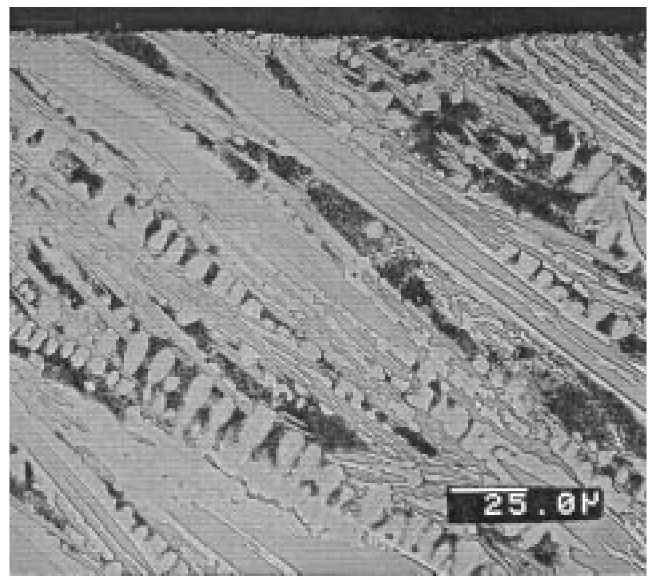

(f)

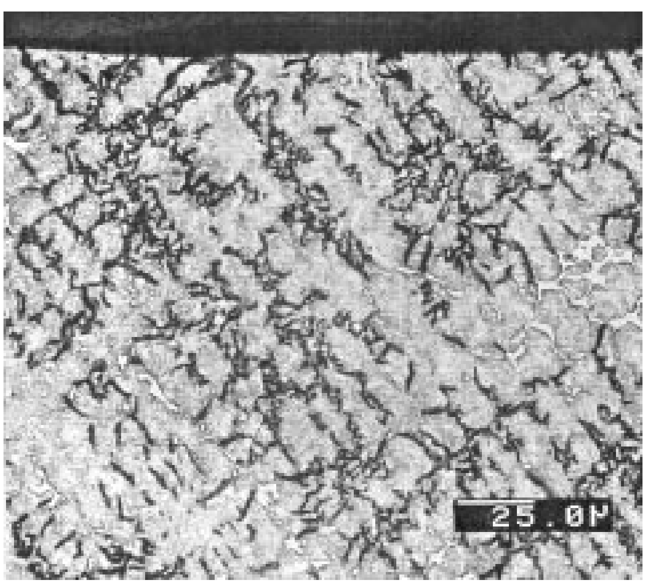

(g)

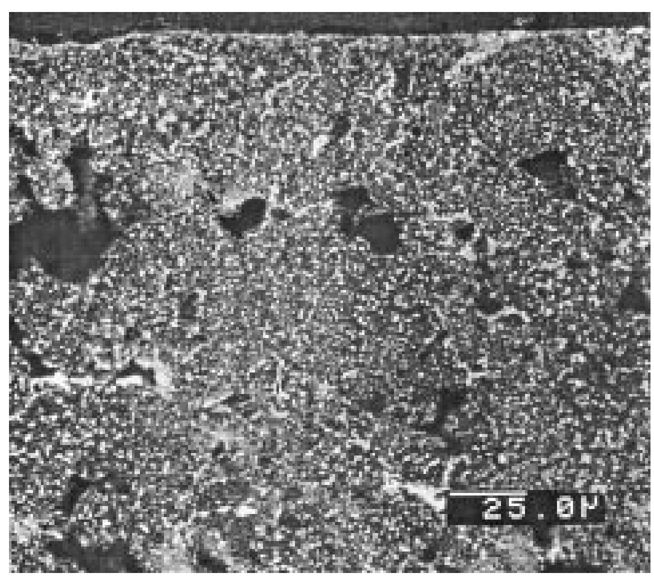

(h)

Fig. 5 (cont.) Microstructures of tested seat inserts at the seat. (e) T 400, Adler's reagent. (f) Eatonite, Marble's reagent. (g) PL 7, 2% nital. (h) PMF 16, Kalling's 2 reagent valve seat surfaces were shear strained (note the radial flow at the seat surface) and oxidized. Tests 24 and 73 (insert materials: Sil XB and PL 7) exhibit a significant amount of oxide film at the valve seat surface (Fig. 6a and b). Test 96 (insert material: Eatonite) displays severe shear strain at the OD of the valve seat wear scar and oxides at the seat (Fig. 6c). An engine-tested valve (a Sil 1 valve against PL 7, M&BP 8178) exhibits oxidation and radial flow at the valve seat (Fig. 6d), similar to that of the rig tests.

Figure 7 shows typical SEM micrographs of seat insert surfaces after rig testing. Surface morphologies of radial grooves inside wear scars suggest that abrasion is one of the wear mechanisms operating on the seat insert surfaces (Fig. 7a and b). “Delamination” (due to severe shear deformation) was another wear mechanism for inserts of Stellite 3 and Eatonite (Fig. 7c and d).

Figure 8 shows typical SEM micrographs of valve seat surfaces after rig testing. Surface morphologies indicate that adhesion (material transfer from insert to valve seat), shear strain, and abrasion were the dominant wear mechanisms on valve seat surfaces.

Figure 9 shows EDX spectra of rig-tested valves and seat inserts inside wear scars. Figures 9(a) and (b) show EDX spectra of Sil 1 valve seats run against T 400 and Stellite 3 inserts, respectively. Molybdenum, cobalt, and tungsten in the spectra indicate that insert materials were transferred to the valve seat

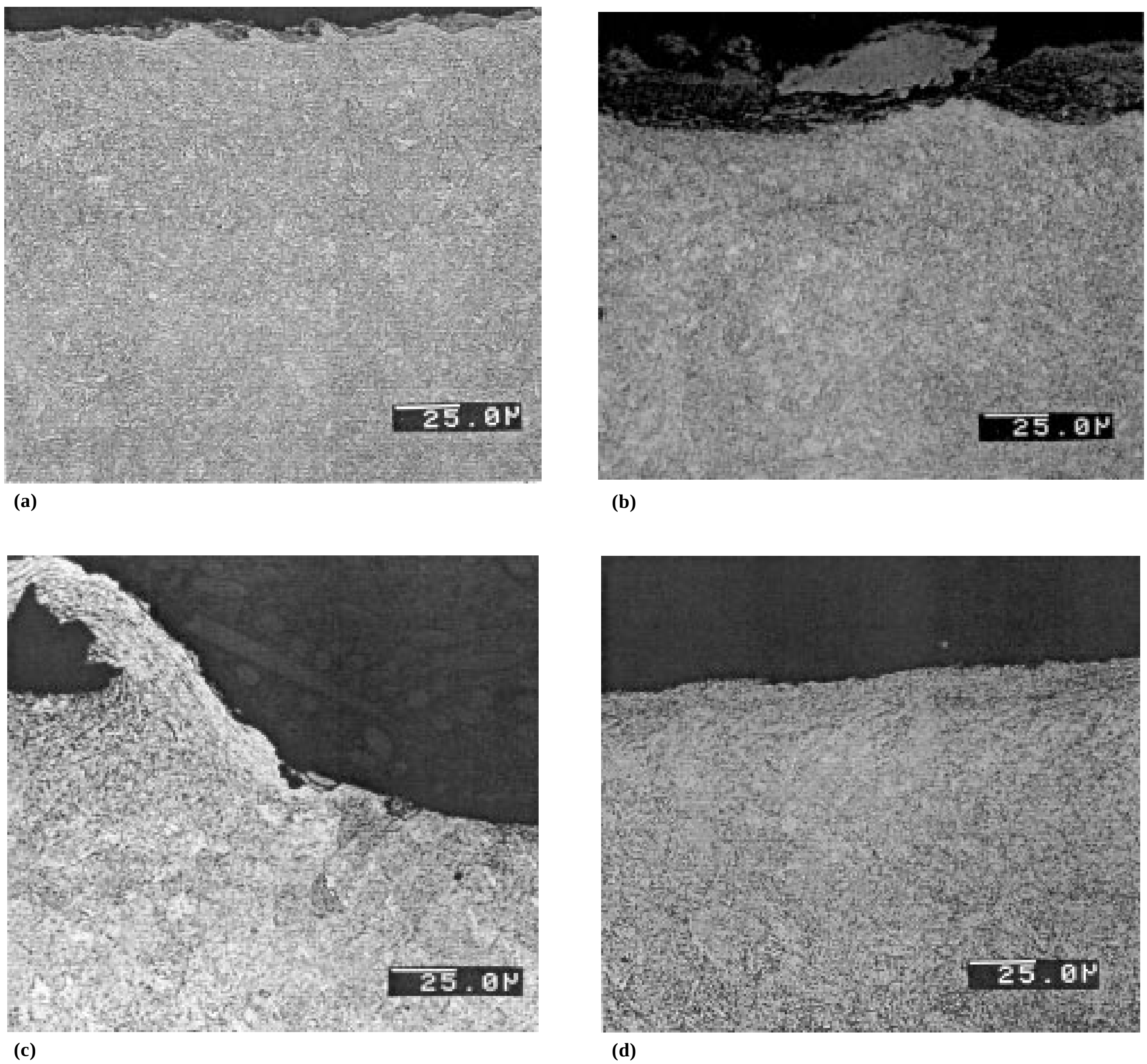

Fig. 6 Microstructures and seat wear morphologies of rig-tested Sil 1 valves and engine-tested Sil 1 valve. Etched in Vilella’s reagent. (a) Rig test, Sil 1/Sil XB. (b) Rig test, Sil 1/PL 7. (c) Rig test, Sil 1/Eatonite. (d) Engine test, Sil 1/PL 7, M&BP 8178

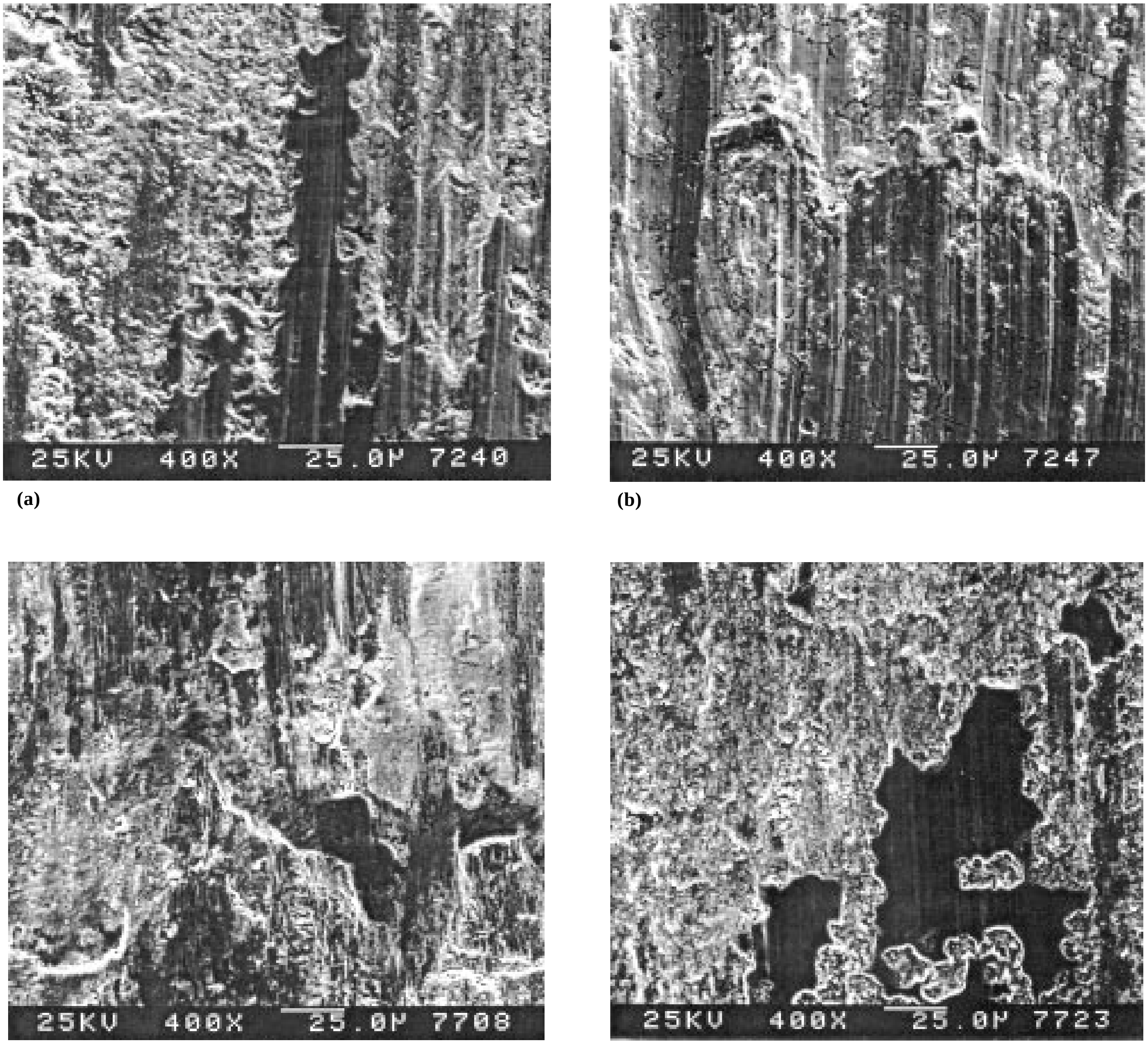

(a) **(b)** **(c)** **(d)**

Fig. 7 SEM micrographs of the seat insert worn surfaces. (a) PMF 16. (b) PL 7. (c) Stellite 3. (d) Eatonite 6

surface during testing. Figures 9(c) and (d) show EDX spectra of seat inserts PL 7 and Eatonite 6. Strong peaks of iron and nickel indicate that adhesion or material transfer occurred from the valve seat to the seat insert.

Examination of the wear, hardness, and microstructures of the valves and seat inserts indicates that material compatibility was critical in valve seat/insert wear reduction. However, there seems little evidence of direct correlation between seat wear/recession (Fig. 4) and material hardness (Table 1), which indicates that the seat wear mechanism was not solely an abrasion or a plastic deformation-controlled process. A large differentiation of valve seat and seat insert hardness was detrimental to the softer counterpart, since abrasion was one of the major seat wear mechanisms. A separate test of a T-400-hardfaced Sil 1 valve against a Sil XB insert resulted in 0.129 ± 0.011 mm wear depth on the valve seat (Table 2). The results indicate that T 400 is not an appropriate valve hardfacing material against a Sil XB insert. They also suggest that harder materials such as T 400 may have higher abrasive wear resistance, but may not necessarily have higher shear strain resistance and adhesive wear resistance.

Microstructural compatibility may also contribute to valve seat wear. Another separate test of a Sil XB valve against a Sil XB insert resulted in 0.028 ± 0.001 mm wear depth on the valve seat (Table 2). The results of a Sil 1 and a Sil XB valve against a Sil XB insert indicate that similar valve and seat insert microstructures may be beneficial in reducing seat wear. The results of a Sil 1 valve against a T 400 insert

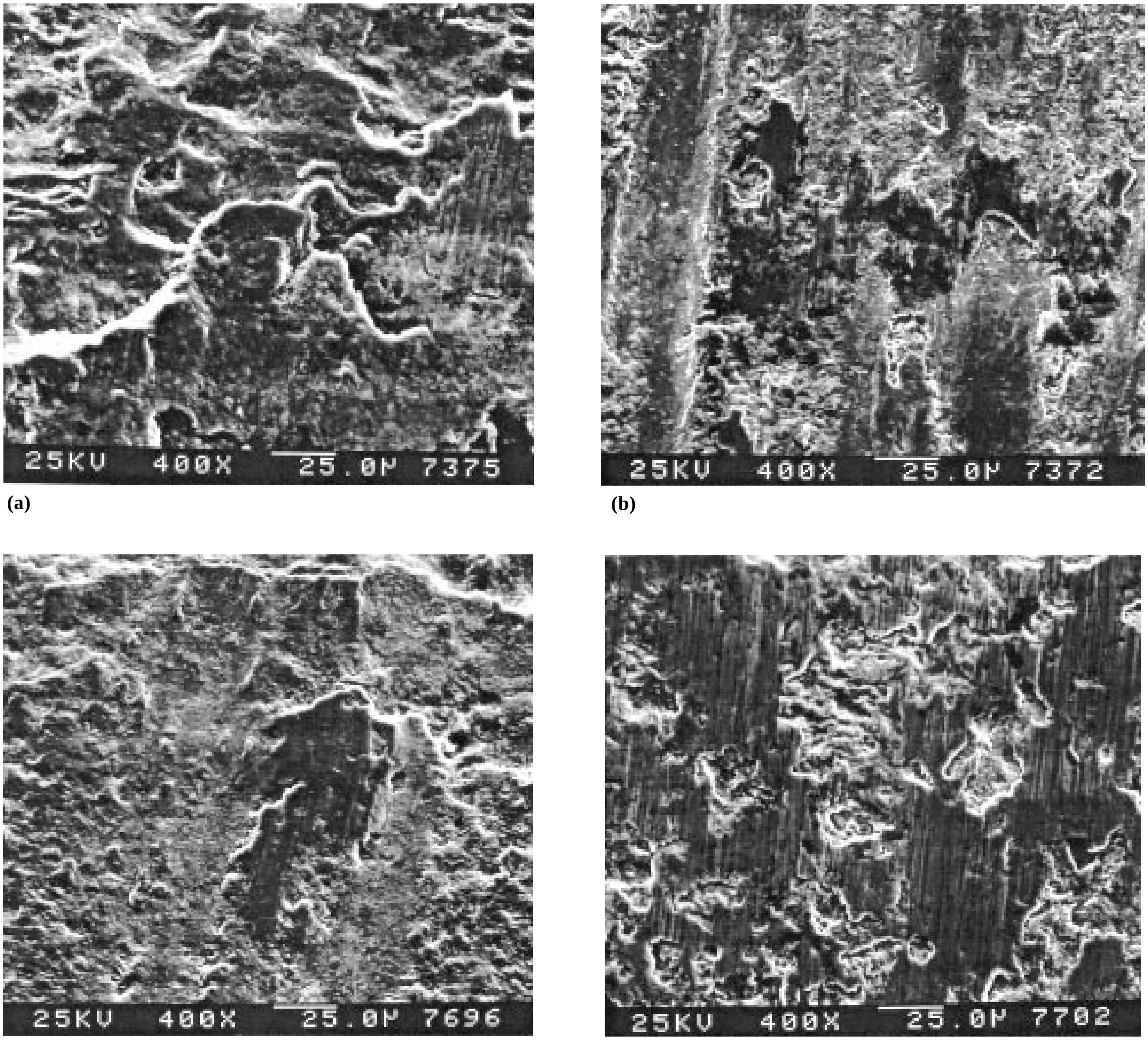

Fig. 8 SEM micrographs of the valve seat worn surfaces. (a) Sil 1/PL 7. (b) Sil 1/Eatonite 6. (c) Sil 1/PL 33. (d) Sil 1/Stellite 3

and a T-400-hardfaced Sil 1 valve against a Sil XB insert also demonstrate that Silchrome and T 400 are not compatible valve and insert materials in reducing valve seat wear, whether T 400 is used as a valve seat hardfacing or as a seat insert.

Three primary wear mechanisms occurred during valve seat wear testing: shear strain, adhesion, and abrasion. Wear of ductile materials was controlled by shear strain when strain at asperity contacts exceeded the critical limits of the materials. The general approach in reducing this type of wear would be to use materials of high yield strength or hardness. Pairing materials with low coefficients of friction can decrease contact stress and strain, thus reducing shear strain-related wear.

Abrasive wear resulted from third-body particles—namely, carbide particles. Grooves on valve seat surfaces are an indication of abrasion. Harder materials have more abrasion resistance. Also, comparable hardness between the valve seat and the seat insert seems to be preferable in reducing abrasive wear problems.

Adhesive wear is characterized by microwelding (or bonding) and subsequent breakage occurring alternately between valve seat and insert surfaces. Some material combinations under certain critical combinations of high stress or poor lubrication are prone to microwelding and breakage, leading to severe adhesive wear. The combination of Silchrome and T 400 is an example. Seat surface oxidation and lubrication can protect the seat from direct metal-to-metal contact, and thus reduce adhesive wear. Oxide films and lubricants can also be beneficial in reducing shear strain-controlled valve seat wear by reducing the coefficient of friction at the seat.

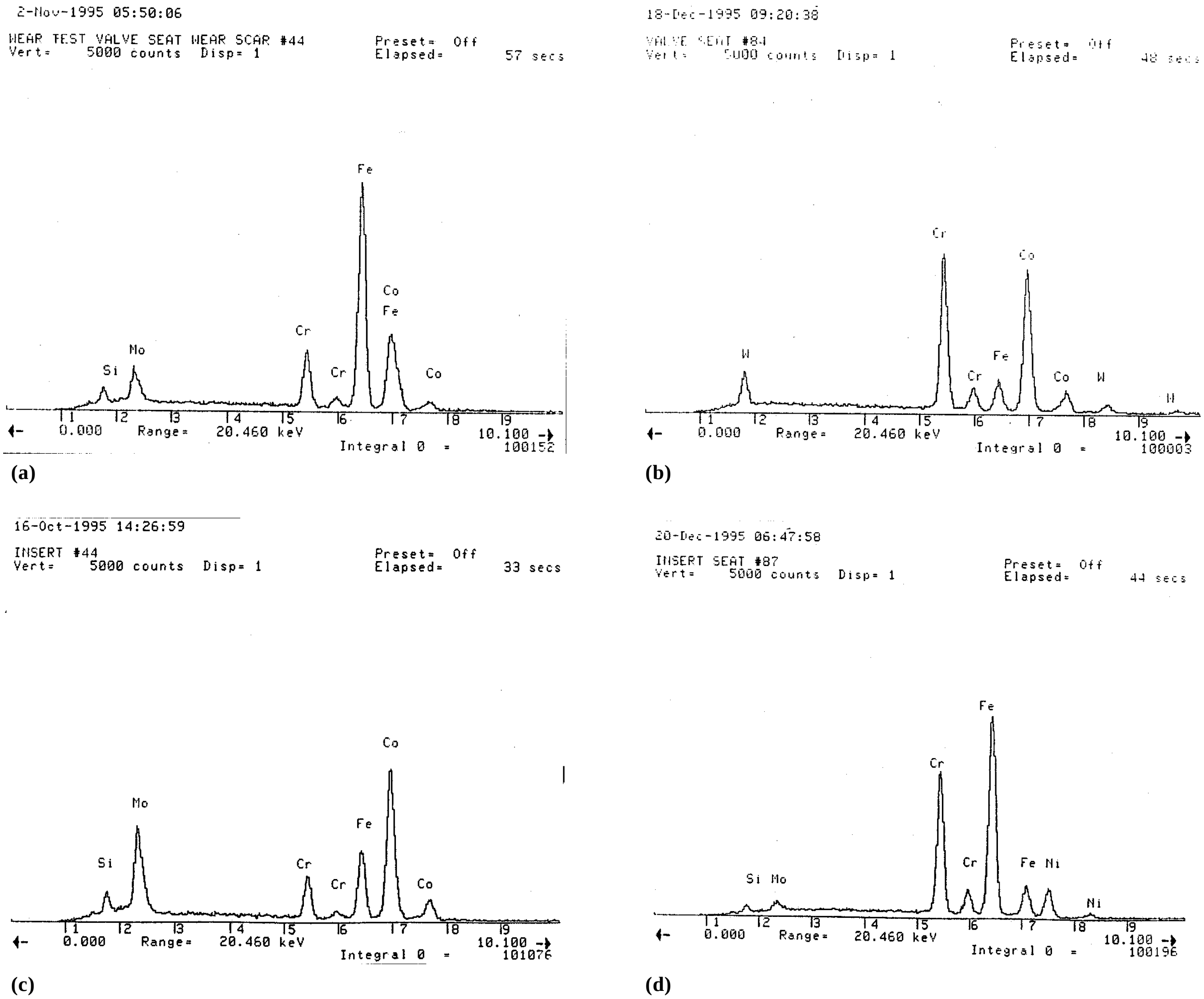

Fig. 9 EDX spectra of valves and seat inserts at the wear scar after testing. (a) Sil 1 valve. (b) Sil 1 valve. (c) T 400 insert. (d) Eatonite 6 insert

4. Conclusions

Sil 1 valves were tested against eight seat insert materials with a valve seat wear simulator; the wear resistance of these combinations was ranked. The combination of a Sil 1 valve against a PL 7 insert had the least valve seat wear, while a Sil 1 valve against a T 400 insert had the highest valve seat wear among the eight combinations of valve/insert materials tested. However, if the industrial standard of total seat recession on both the valve and the insert is considered, the combination of Sil 1 valve/Eatonite 6 insert had the least total seat recession. Sil 1 valves against T 400, PL 7, and Eatonite inserts had severe seat recession.

Wear mechanisms of Sil 1 valves and seat inserts were a complex combination of adhesion, shear strain, and abrasion. Shear strain (or radial flow) was an important intake valve seat wear mechanism based on microstructural analysis of radially sectioned valve seats and 2-D and 3-D worn seat profiles. The oxide films formed during testing played a significant role. They prevented direct metal-to-metal contact and reduced the coefficient of friction on the seat surfaces, thus reducing adhesive and deformation-controlled wear.

Acknowledgments

The authors thank E. Hurlbert, S. Pattinson, and B. Trine at Eaton Corporation, Engine Components Operations, for their technical assistance.

References

1. K. Zinner, "Investigations Concerning Wear of Inlet-Valve Seats in Diesel Engines," ASME Paper No. 63-OGP-1, American Society of Mechanical Engineers, 19-23 May, 1963
2. K.L. Brown and N.D. Bohner, "Valve Wear, Statistically Speaking," ASME Paper No. 77-DGP-6, American Society of Mechanical Engineers, 1977

3. S.L. Narasimhan and J.M. Larson, "Valve Gear Wear and Materials," SAE Paper No. 851497, Society of Automotive Engineers, 1985
4. R. Van Dissel, G.C. Barber, J.M. Larson, and S.L. Narasimhan, "Engine Valve Seat and Insert Wear," SAE Paper, No. 892146, Society of Automotive Engineers, 1989
5. Y.S. Wang, S.K. Schaefer, C. Bennett, and G.C. Barber, "Wear Mechanisms of Valve Seat and Insert in Heavy Duty Diesel Engines," SAE Paper No. 952476, Society of Automotive Engineers, 1995
6. T.N. Tunnecliff and L.F. Jenkins, "Why Valves Succeed," SAE Paper 249B, Society of Automotive Engineers, 1960
7. R. Zhao, G.C. Barber, Y.S. Wang, and J.E. Larson, Wear Mechanism Analysis of Engine Exhaust Valve Seat with a Laboratory Simulator, *STLE Trans.*, Vol 40 (No. 2), 1997, p 209
8. M.J. Malatesta, G.C. Barber, J.M. Larson, and S.L. Narasimhan, Development of a Laboratory Bench Test to Simulate Seat Wear of Engine Poppet Valves, *Tribol. Trans.*, Vol 36 (No. 4), 1993, p 627